Revista Geológica de América Central, 43: 119-135, 2010
ISSN: 0256-7024

GROUND PENETRATING RADAR IMAGING OF TEPHRA STRATIGRAPHY ON POÁS AND IRAZÚ VOLCANOES, COSTA RICA

IMÁGENES CON EL RADAR DE PENETRACIÓN TERRESTRE EN LA TEFROESTRATIGRAFÍA RECIENTE DE LOS VOLCANES POÁS E IRAZÚ, COSTA RICA

Sarah Kruse[1]*, Raul Mora-Amador[2], Carlos Ramírez[2]
& Guillermo E. Alvarado[2,3]

[1]Department of Geology, University of South Florida
[2]Escuela Centroamericana de Geología, Centro de Investigaciones en Ciencias Geológogicas, Universidad de Costa Rica
[3]Área de Amenazas y Auscultación Sísmica y Volcánica, Instituto Costarricense de Electricidad (ICE)
*Autora para contacto: skruse@usf.edu

(Recibido: 10/08/2010; aceptado: 08/11/2010)

ABSTRACT: Ground penetrating radar (GPR) has been shown to be a useful tool for mapping geometry and thicknesses for volcanic fall, surge, granular flow, and lahar deposits. However, the success of GPR surveys is highly dependent on soil properties and the nature of stratigraphic layering. The efficacy of the method at a given site can be difficult to predict. Small-scale (10s to 100s of meters) test surveys with ground penetrating radar show that geologic features of interest can be resolved to depths up to 20 m on both Poás and Irazú volcanoes in Costa Rica. The antenna frequencies used in this pilot study, 50 MHz, 100 MHz, and 200 MHz, produce wavelengths too long to resolve most individual layers (mm's to cm's thick) in the near-surface tephra fall and surge deposits. However, these GPR profiles clearly show the attitude of beds and resolve some distinct contacts at depth, particularly the base of the 1963-1965 intracrater deposits on Irazú. On Irazú GPR profiles also confirm field observations that 1963 surge deposits thin consistently with distance from the crater rim, while packages from 1723 and older show uniform thicknesses or increasing thickness with distance from crater rim, suggesting reworking or reverse flow of surges returning from the Playa Hermosa caldera wall. On Poás, bright reflectors are present at depths below 2 m on near-vent profiles, but the lack of nearby stratigraphic observations precludes geological interpretation. The test profiles on both volcanoes also clearly show diffractions produced by blocks on the order to 5 cm or more in diameter embedded in the surficial deposits, as well as evidence of sag beneath blocks. Resolution of blocks decreases with depth, presumably due to both the inherent loss in lateral resolution with wave travel distance and to clearly observed dispersion (loss of high frequencies). Future studies, particularly with higher frequency antennas on Poás, could be useful for tracking depositional units between exposures, and for resolving the distribution of blocks or bombs in deposits in the uppermost few meters.
Keywords: Ground penetrating radar, tephrastratigraghy, Poás, Irazú, Costa Rica.

KRUSE, S., MORA-AMADOR, R., RAMÍREZ, C. & ALVARADO, G.E., 2010: Ground penetrating radar imaging of tephra stratigraphy on Poás and Irazú volcanoes, Costa Rica.- Rev. Geol. Amér. Central, 43: 119-136.

RESUMEN: El Radar de Penetración Terrestre (GPR) ha demostrado ser una herramienta útil para el mapeo geométrico y el espesor de depósitos volcánicos de caída volcánica, oleadas, flujos granulares y lahares. Sin embargo, el éxito de estudios con GPR es muy dependiente de las propiedades del suelo y la naturaleza de las capas estratigráficas. La utilidad del método en un sitio particular puede ser difícil de predecir. A pequeña escala (decenas a centenas de metros), los estudios de la prueba con el GPR muestra que los rasgos geológicos de interés pueden ser resueltos hasta una profundidad de 20 m en ambos volcanes de Costa Rica, Poás e Irazú. Las frecuencias de las antenas usadas en este estudio piloto, 50 MHz, 100 MHz, y 200 MHz, producen longitudes de onda demasiado largas para identificar la mayoría de las capas individuales (mm a cm de espesor) en los depósitos de caída y oleadas cercanos a la superficie. No obstante, estos perfiles de GPR claramente muestran las características de las capas e identifica algunos contactos distintivos a profundidad, particularmente la base de los depósitos intracratéricos de las erupciones del Irazú en 1963-1965. En el Irazú, los perfiles de GPR también confirman observaciones del campo que los depósitos de oleadas de 1963-65 se adelgazan de forma consistente con la distancia al borde del cráter, mientras que los paquetes de 1723 y más antiguos, muestran un espesor uniforme o un espesor creciente con la distancia del borde del cráter, sugiriendo un re-trabajo o flujo reverso de las oleadas que se devuelven al chocar contra la pared de la caldera de Playa Hermosa. En el Poás, las reflecciones significativas se presentan a profundidades por debajo de 2 m en los perfiles cerca del cráter principal, pero la falta de observaciones cercanas en la estratigrafía evita una mejor interpretación geológica. Los perfiles de prueba en ambos volcanes también muestran claramente difracciones producidas por bloques en el orden a 5 cm o más en diámetro enclavados en los depósitos superficiales, así como la evidencia de deformación bajo los bloques. La resolución de los bloques disminuye con la profundidad, presumiblemente debido a la pérdida inherente en la resolución lateral con la distancia de viaje de la onda y a la dispersión claramente observada (pérdida de altas frecuencias). Estudios futuros, particularmente con antenas de más alta frecuencia en Poás, podrían ser útiles para correlacionar las unidades depositacionales entre los diferentes afloramientos y para visualizar la distribución de bloques o bombas en depósitos en los primeros metros.
Palabras clave: Radar de penetración terrestre, tefroestratigrafía, Poás, Irazú, Costa Rica.

INTRODUCTION

Mapping of near-surface stratigraphy on volcanoes is useful for understanding recent eruptive styles and volumes and for resolving the degree to which material is mobilized following eruptions by mass movement and erosion. Ground penetrating radar has proven a useful tool for all of these tasks, particularly for extending subsurface imaging between outcrops, and extending resolution to three dimensions.

Poás volcano

Poás (2708 m a.s.l.) is a complex stratovolcano with a subconic irregular shape and 3 principal edifices, the main (or active) crater, the Botos cone, and the von Frantzius cone. Of these only the main crater has been historically active. The uppermost deposits around the main crater are products of this historical activity. In 1834 there was a strong eruption accompanied by loud underground detonations, and deposits extended 40 km from the volcano. Another major eruption occurred on January 25, 1910. The ash column rose to an estimated height of 4000 m, then spread outward and upward till it reached a height of approximately 8000 m (Rudin et al., 1910). Deposits from the 1910 eruption are identifiable in the field and in trenches. Finally, in 1953 a violent explosion led to the temporary disappearance of the existing crater lake (Monestel, 2004). Relatively violent eruptions continued until 1955.

Irazú volcano

Irazú (3432 m a.s.l.) is a basaltic andesite shield volcano. The surficial deposits that are the subject of this study were produced from its major recent eruptions, which occurred in 1723 and 1963-1965. These eruptions caused significant ash fall, and subsequent lahars. Close to the active

vent, deposits from these events include a mixture of surge and fall, with surge deposits predominating (Alvarado, 1993; Alvarado et al., 2006).

GPR studies of volcano stratigraphy

GPR methods are similar to seismic methods, but utilize electromagnetic waves rather than elastic waves. Reflection profiles are traditionally collected by moving a single transmitter-receiver pair (kept at a fixed separation) along a transect. To determine wave velocities at selected locations, common midpoint (CMP) surveys are conducted by gathering data over a range of antenna separations. Alternatively, in environments with point sources such as volcanic blocks, the velocities can be determined from analysis of the form of diffractions. In volcanic deposits, velocities are controlled principally by porosity, water content, and matrix composition (presence of organics, clays, etc.). In relatively uniform fall and flow deposits, returns are associated with contacts that mark the distinct changes in porosity and lithology that are occur when eruption style (and deposited material) changes, and with paleosols or weathering horizons that form during quiescent periods. In more chaotic deposits lacking coherent layering, GPR records show scattering from individual blocks and porosity boundaries. A number of studies have capitalized on GPR's capabilities in volcanic settings (Russell & Stasiuk, 1997; Cagnoli & Russell, 2000; Rust & Russell, 2000, 2001; Cagnoli & Ulrych, 2001a, 2001b; Miyamoto et al., 2005; Chow et al., 2006; Gómez-Ortiz et al., 2006; Grimm et al., 2006; Heggy et al., 2006).

Although GPR surveys can detect the presence of very thin units (mm-cm thickness), the method cannot resolve the thickness of beds thinner than approximately 1/4 of the radar wavelength (e.g. Guha et al., 2005). In practice, vertical resolution limits in volcanic deposits (velocities ~0.04-0.14 m/ns) range from ~20-70 cm for 50 MHz antennas and from ~5-18 cm for 200 MHz antennas. Where strata are thinner than this resolution limit, the GPR profile in general yields an image that shows the attitude of beds, without a one-to-one relationship between reflections events and contacts in the subsurface.

Depth of penetration depends principally on the conductivity of the deposits, which varies considerably with lithology (i.e. clay content), antenna frequency, and scattering arising from deposit heterogeneity. Very recent volcanic deposits are typically highly resistive, so where deposits are internally relative uniform (little scattering), it is possible to achieve penetration of tens of meters for 50 MHz antennas, and up to 5 m or more with 200 MHz antennas.

RESULTS AND DISCUSSION

At all sites described here, test surveys were run with 200 MHz, 100 MHz and 50 MHz antennas. In each case, we present the results with the antenna frequency that provides the most useful combination of spatial resolution and depth of penetration. Profiles are presented without topographic corrections as topographic variation along lines was negligible in comparison with the depth variability in strata imaged.

GPR on Poás

Several GPR profiles were conducted in April and June 2004 to test the capabilities of this method for resolving the stratigraphy of superficial ash deposits high on the flanks of Poás, and near an older crater (Figure 1). The first test was conducted on an open meadow known as "Potrero Grande" 2 km south of the active crater, adjacent to the site of a 1.5 m-deep trench (Figure 2). The stratigraphy in the trench was mapped by Mora-Amador (2010). GPR data were collected with a Sensors and Software PulseEKKO 100 system with 200 MHz unshielded antennas, a transmitter-receiver offset of 0.5 m, a 16 or 32-fold stack and a trace interval of 10 cm. Data were processed with the ReflexW program from Sandmeier Software. The data were dewow filtered, static shifted, gained with an energy decay gain, corrected for source-receiver offset, and finally migrated with a diffraction stack constant velocity migration. The velocity for the migration was determined from an expanding-spread common-midpoint survey collected along the profile

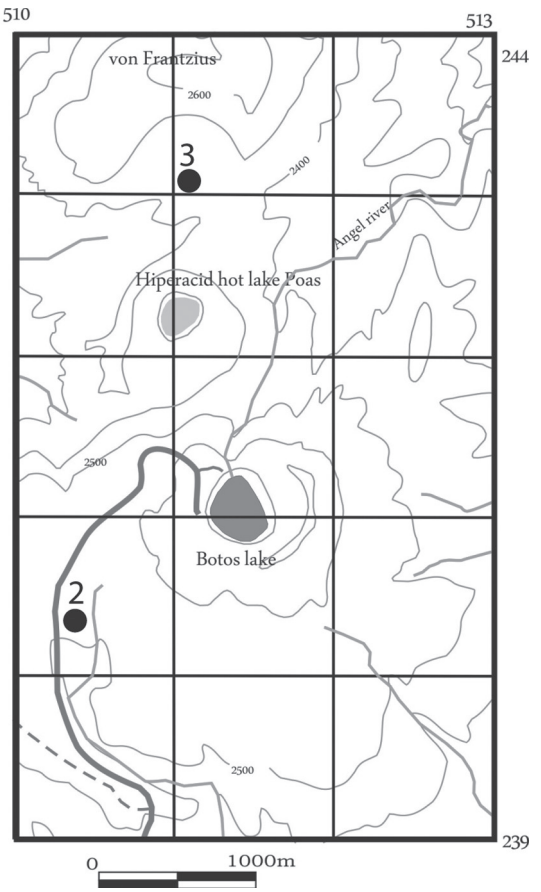

Fig. 1: Map of the craters on the Poás volcano. Solid circles labeled 2 and 3 indicate locations of GPR profiles shown in Figures 2 and 3, respectively. The profile lengths themselves are smaller than the circles.

that showed remarkably uniform velocities with depth, with interval velocities from ranging 0.043 to 0.047 m/ns over the 6 m imaged.

The very low wave velocities presumably reflect a very high degree of water saturation in the ash deposits, as the data were collected between periods of heavy rainfall. The velocities are of course also a function of lithology, and these deposits may be rich in clay because of their phreatic nature. (The clay content, however, does not cause excessive attenuation of the radar signal.) The wavelength of the 200 MHz pulse shortens in the slow velocity material to ~ 15 cm. This is still long, however, compared to the thickness of most distinct units identified in the trench (Mora-Amador, 2010), with the result that the much of the GPR profile represents a filtered version of the subsurface, where reflected energy from various horizons overlaps in time. Figure 2 shows that in the uppermost 1.5 m, 18 distinct soil horizons were identified by trenching (Mora-Amador et al., 2010), but there are only 4 distinct higher-amplitude reflection events from this same depth range. It is clear that to follow the stratigraphy of individual ash deposits (such as the 1910 or 1953 deposits, which are only ~3 cm thick at this site), higher-frequency antennas, such as 800 MHz, would be necessary.

Despite the limited resolution, there are several interesting features in the 200 MHz GPR profiles of the ash and underlying strata. The reflecting horizons in the uppermost 3 m are sub-parallel to the surface over the 19-m profile shown in Figure 2, as well as over 50 m of profiles run in various orientations at this test site. The attitude of the reflection events is consistent with the form expected for pyroclastic flows or tephra fall deposits that blanket underlying deposits. Between 3 to 4 m depth, there is a distinctly different reflecting horizon (A on Figure 2), that shows a depth variation and roughness not seen in the shallow returns. The unmigrated profile (left side, Figure 2) shows diffractions along this contact, which are focused reasonably well in the migrated image (right side, Figure 2). The jaggedness of the reflector at 3-4 m depth suggests a flow with distinctly different rheology, whose rough upper surface was preserved. This horizon (A on Figure 2) may represent an unconformity that separates recent unconsolidated tephra deposits from older (>10,000 year B.P.) more consolidated tephra deposits.

The test profiles conducted at this site indicate that penetration depths of radar waves are sufficiently deep that high-frequency antennas (e.g. 800 MHz) should capture reflections from the uppermost 1-2 m, while possibly resolving individual distinct ash deposits (such as the 1910). The continuity of reflectors in the test radar record (Figure 2) suggests that GPR could be a valuable tool for tracking continuous fall and surge deposits on the flanks of the active crater, where access permits.

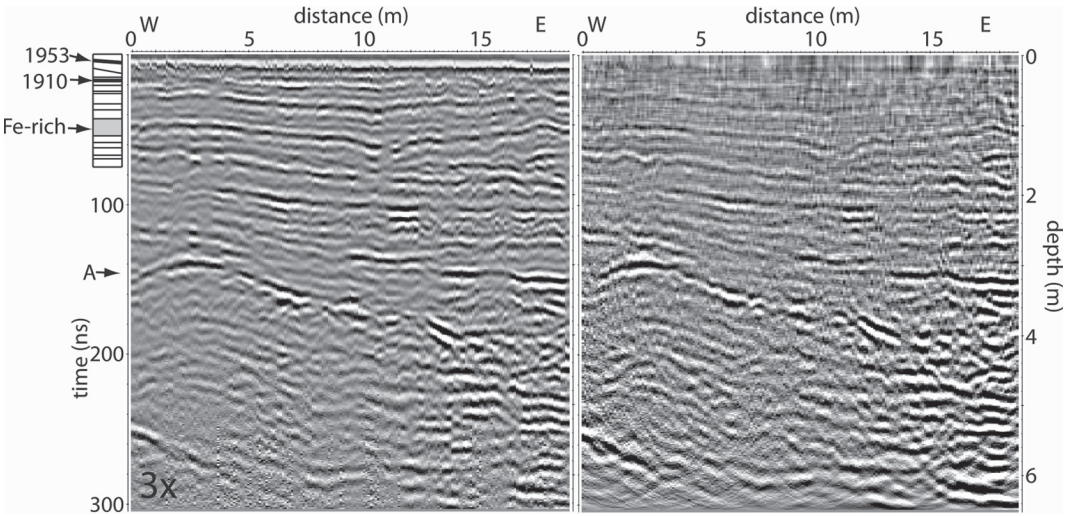

Fig. 2: Trench stratigraphy and GPR profile bearing east that passes just north of trench at x = 2 m. (Location shown on Figure 1.) Upper left: trench stratigraphy from Mora-Amador et al. (2004). All horizontal/dipping lines represent contacts between distinct ash units. Dipping lines represent the range of depths reported for a given contact. Units shown in black are dated ash deposits from 1910 and 1953 eruptions. Gray unit is characterized by discontinuous Fe-rich layers that might be expected to produce strong GPR reflection. Middle: GPR profile with 3x vertical exaggeration, processed as described in text but not migrated. "A" marks a horizon with depositional characteristics distinct from the overlying ash deposits, perhaps an unconformity between older (>10,000 y B.P.) tephra and younger less consolidated tephra deposits. Right: same profile, migrated with constant velocity of 0.043 m/ns derived from nearby common midpoint profile.

A second set of test lines were run in April 2004, 800 m north of the active crater, near von Frantzius crater (Figure 3). Here a nearby stream cut shows ash with small (a few to 10s of cm) block inclusions. Ash units from individual eruption events are not clearly identifiable, instead contacts between ash units are visible primarily as changes in the nature of the inclusions. The profile shows 200 MHz GPR is relatively insensitive to such contacts. (Another test profile with 100 MHz antennas gave similar results, with poorer resolution of the 30 cm - 1 m depth range.) Only a single sub-horizontal reflector is observed at ~40 cm depth. Below that, the only significant energy return is from diffractors and intermittent reflectors, principally below 2.5 m. Attempts to migrate the data with a variety of velocity models were not successful at clarifying the image. This suggests that the blocks and other features are fundamentally three-dimensional (as expected) and that the velocity structure may be quite complex.

GPR appears to have limited utility as a method for tracking these older deposits, where contacts between units are not defined by clear porosity changes, as seen in the nearby stream cut.

GPR on Irazú

Data were collected at two sites at the crater rim. The first site (profiles A and B on Figure 4) is the outside southwest-dipping flank of an elongate cone that formed on the crater rim during the 1963-65 eruptions (Figures 5 and 6). These profiles were acquired in July 2004. The short profile lengths made it practical to acquire data with a 128-fold stack. Profile A was acquired with 200 MHz antennas and a 10-cm trace spacing; Profile B with 100 MHz antennas and a 25-cm trace spacing. Velocities were computed from common mid-point surveys conducted just after the profiles, near the midpoints of the profiles. Interval velocities over packages between velocity picks were relatively uniform (ranges of 0.01-0.02 m/ns), and an average value of 0.09 m/ns was used for time to depth conversions on these profiles. Data were processed with a combination of Sensors and

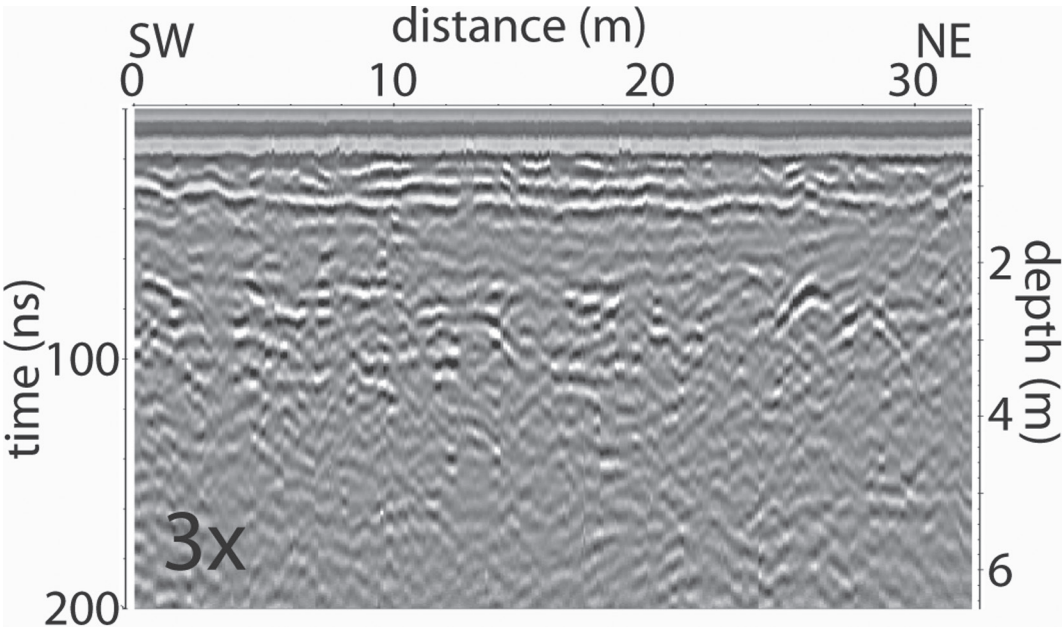

Fig. 3: GPR profile on exposed portion of older crater north of Poás. Location shown on Figure 1. This site lacks layers with distinct porosity contrasts, and below 1 m returns represent a complex pattern of diffractions and semi-coherent reflections from units with cm-diameter blocks embedded in a finer, heterogeneous matrix. 3x vertical exaggeration.

Software pulseEKKO software and original Matlab algorithms. Data were dewow filtered, static shifted, gained with AGC, corrected for antenna offset, and waveform data travel times were converted to depth assuming a constant velocity. The data are shown in unmigrated form (Figures 5 and 6) to illustrate the distribution of diffraction hyperbolas generated by bombs or blocks.

The complex stratified tephra deposits within this cone are termed "Intracrater Deposits" by Alvarado (1993). He divides them into four intracrater explosive units, ICEU-1 through ICEU-4, separated by erosive contacts. Figure 7 shows a tentative correlation between the GPR profiles and the stratigraphy mapped by Alvarado (1993). Because of the fine-scale layering within the ICEU units, a one-to-one relationship between ICEU boundaries and strong radar returns would not be expected. Nevertheless, the resolution and continuity of the GPR stratigraphy are good enough that stratigraphic features in the GPR profiles are presumably representative of features within or at the boundaries of the ICEUs. An exceptionally strong reflector seen in the 100 MHz records at 20 m below surface (Figures 6 and 7) clearly correlates well with local depth to the base of the 1963-65 deposits.

Several characteristics of the GPR profiles over the intracrater deposits are worth noting. First, it is clear from examination of profiles A and B (Figures 5 and 6) that diffraction hyperbolas are a significant part of the energy returned from shallower depths (<~ 100 ns travel time, or ~4.5 m depth). In contrast later returns appear as strong subhorizontal reflecting horizons separated by relatively transparent zones. However, out-

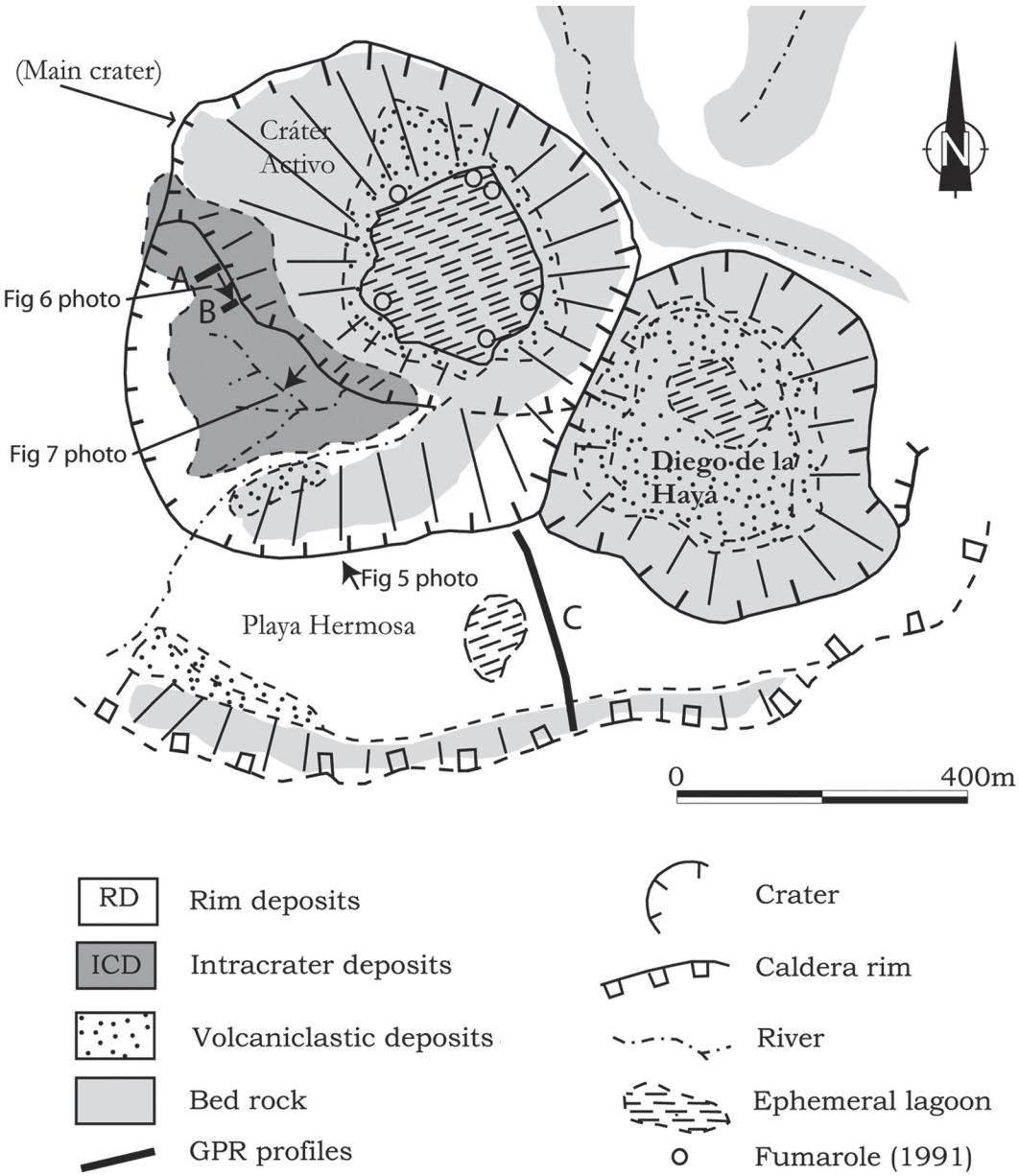

Fig. 4: Geologic map of Irazú volcano craters modified from Alvarado (1993). Thick lines show locations of GPR profiles discussed in this paper. Thick arrows mark locations and direction from which photos in Figures 5, 6, and 7 were taken.

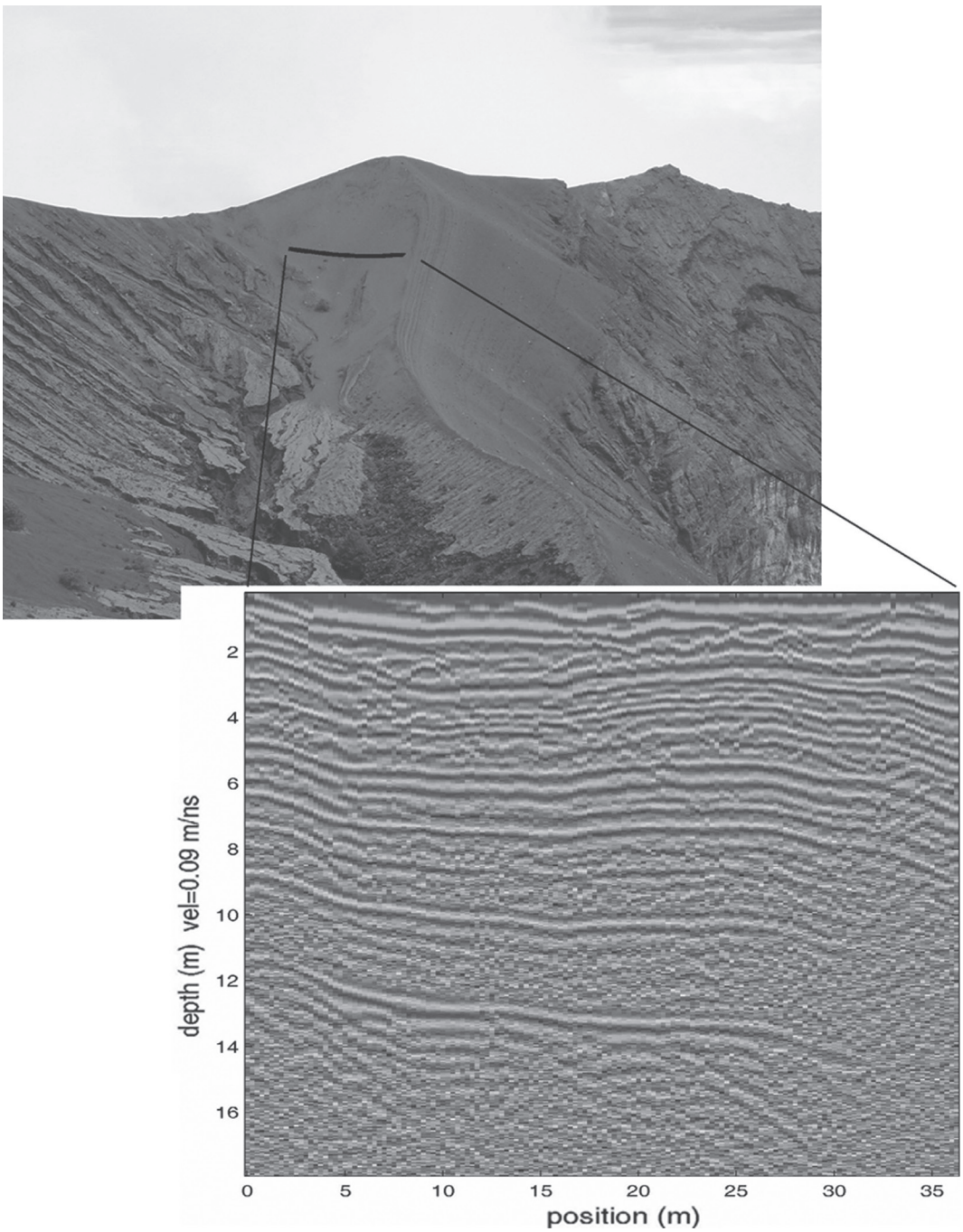

Fig. 5: GPR Profile A on Irazú intracrater 1963-1965 deposits. 200 MHz antennas. Profile location and site and direction of photo are shown on Figure 4. Photo shows the cone that formed on the western rim of the active crater during the 1963-1965 eruption. Profile was run at roughly uniform elevation.

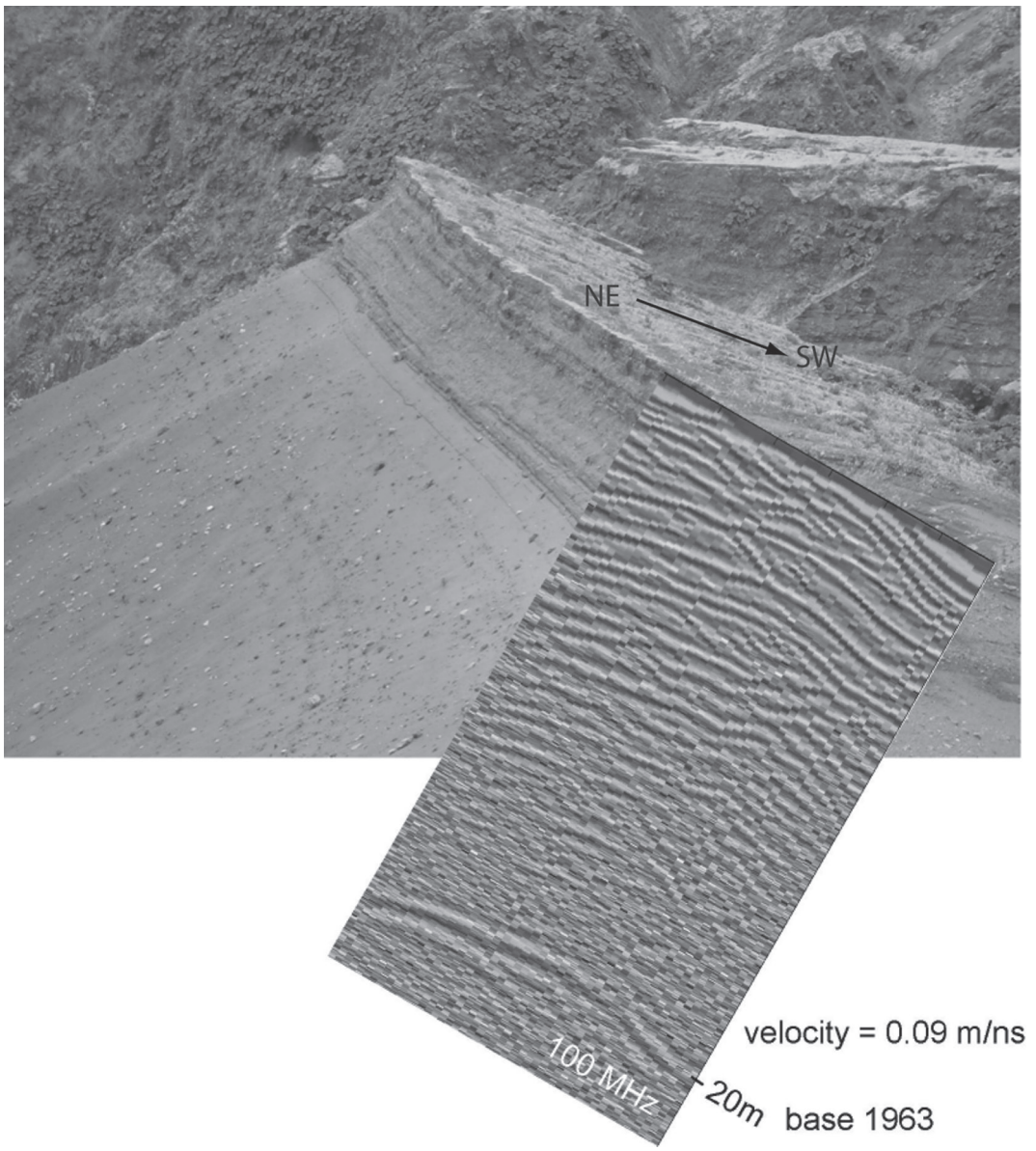

Fig. 6: GPR Profile B on Irazú intracrater 1963-1965 deposits. 100 MHz antennas. Profile location and site and direction of photo are shown on Figure 4. A strong GPR reflector correlates with the base of the 1963 deposits.

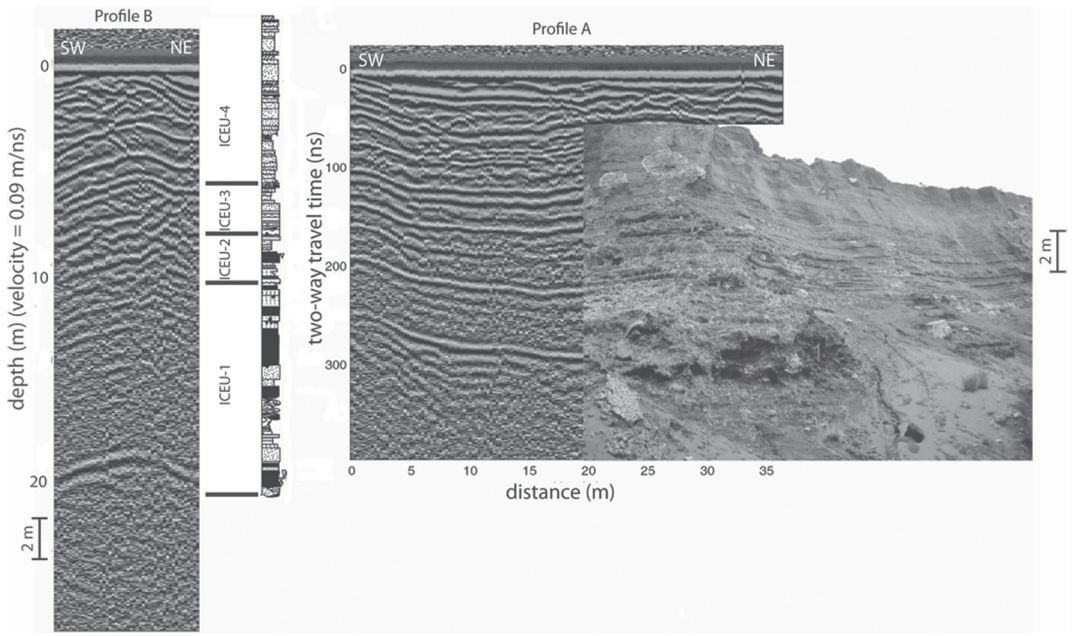

Fig. 7: Comparison of GPR profiles A and B (see Figure 4 for location) with stratigraphic column of 1963-1965 "Intracrater Deposits" from Alvarado (1993). The correlation between the basal 1963 contact and the strong GPR reflection at ~410 ns is well defined; further work is needed for definitive correlations between individual reflection events and the erosional surfaces separating Alvarado's ICEUs (intracrater explosive units, red numerals in photograph). The outcrop photo is taken at a stream cut ~100 m south of profile B where the uppermost horizons visible on the GPR lines have probably been eroded (see Figure 4 for location). The absence of diffraction hyperbolas in the lower portions of the GPR profiles may be due in part to wave dispersion (Figure 8).

crops at stream cuts near the radar lines show that larger inclusions (blocks, bombs a few cm to > 20 cm diameter) are pervasive throughout all four ICEUs. The absence of diffraction hyperbolas in the later parts of the radar traces could be due to the decreasing lateral resolution with wave travel distance. The absence also makes sense if there is significant dispersion, or loss of high frequencies, in the radar wave as it travels through the sediments (e.g. Irving & Knight, 2003). The lower-frequency energy that arrives at greater depths corresponds to longer wavelengths, which do not undergo diffraction from smaller clasts. In fact, time-frequency analysis of a trace from Profile B shows that there is significant and relatively uniform dispersion of the radar wave (white line on Figure 8). While the dominant frequency near the surface is about 100 MHz (wavelength ~90 cm), at 20 m depth (base of 1963 deposits) it is about 60 MHz (wavelength ~1.5m). This dispersion is greater than that found in many sedimentary environments with more uniform grain size distributions. The dispersion presumably represents a combination of both intrinsic attenuation and scattering concentrated at the higher frequency components of the wave.

A second set of GPR profiles was run on the Playa Hermosa of Irazú volcano, believed to be a remnant crater filled with deposits from subsequent eruptions. One of the acquired profiles is interpreted in this paper (Profile C on Figure 4; Figure 9). Data were acquired with 200 MHz antennas and a 10-cm trace interval. Velocities derived from CMPs conducted mid-profile immediately following the surveys show best-fitting value of 0.065 m/ns. The deposits imaged in these profiles are mapped and described as "Rim Deposits" by Alvarado (1993). The lowest units captured by GPR are verified in outcrop as a hydrothermally altered package that pre-dates 1723 deposits; the uppermost strata are a set of surge packages produced in the 1963-1965

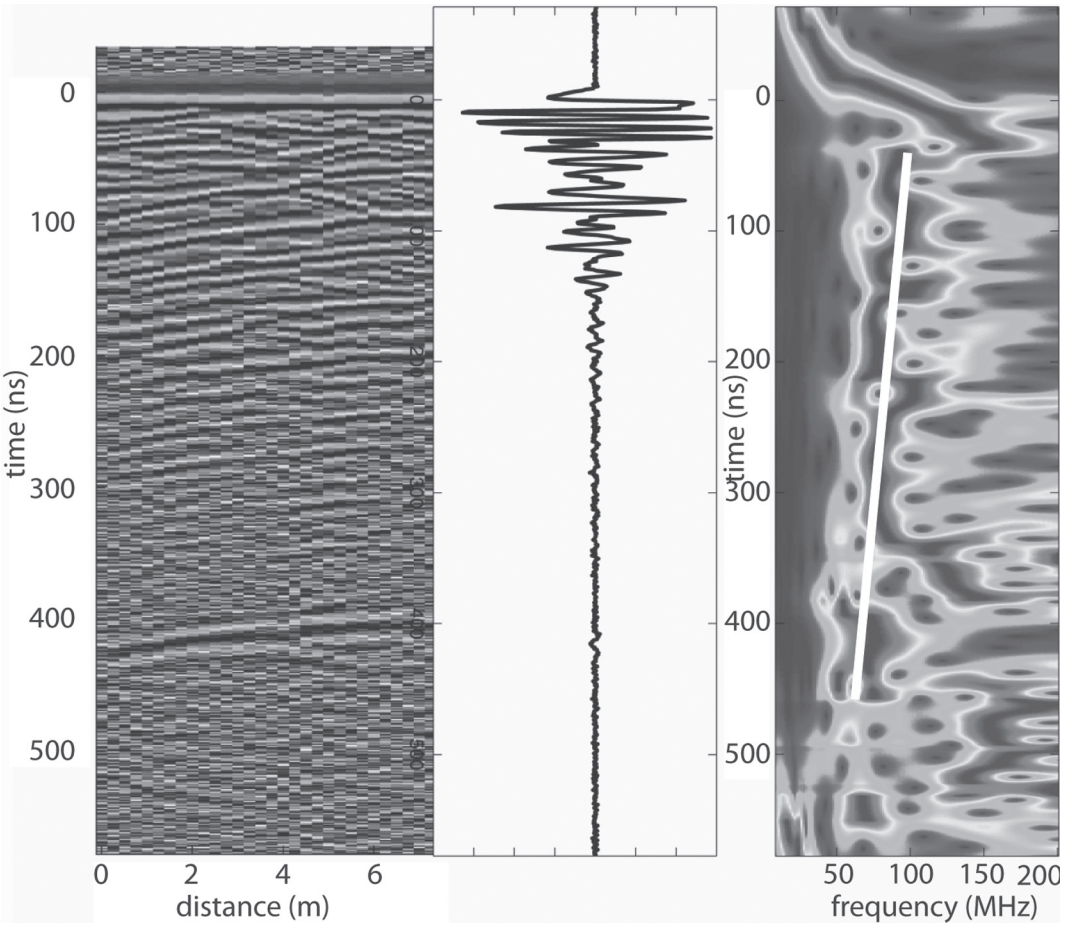

Fig. 8: Time frequency analysis of the trace located at x = 7 m on profile B (location shown in Figure 4). Left: The western 7 meters of profile B. The right edge of this profile is the trace shown in the center (without gain). The right plot shows relative energy as a function of frequency and with time throughout the trace. The time-frequency analysis was computed using the S-transform of Stockwell et al. (1996). Reds mark frequencies at which energy is concentrated. Bands of red at high frequencies late in the record represent noise rather than signal. The white line illustrates the relative uniform decrease in central frequency of the return as a function of time, as high frequencies are selectively attenuated and/or scattered.

eruption sequence. At this location the 1963-65 surge deposits are some 2 m thick (Alvarado, 1993). Within these deposits are numerous strata with thicknesses much less than the ¼ wavelength resolution limit (8 cm for 200 MHz at 0.065 m/ns), so the radar records represent an interference pattern of many reflections, as described above for the Poás profiles.

Despite the resolution limitations useful information on the attitudes and thicknesses of combined packages of strata can be derived from the GPR profiles. For example, 6 strong GPR reflection events were selected from the GPR record (Figure 9), and arrival time picks were made on a consistent part of the phase of each arrival. The corresponding depths were computed using best-fitting the CMP-derived velocities (Figure 10). Because the same phase was not used for each event (in some cases picks were made on positive polarity peaks, in some on negative) the absolute value of the thickness of each identified package between reflection events is only approximate, but changes in thickness across the profile are significant.

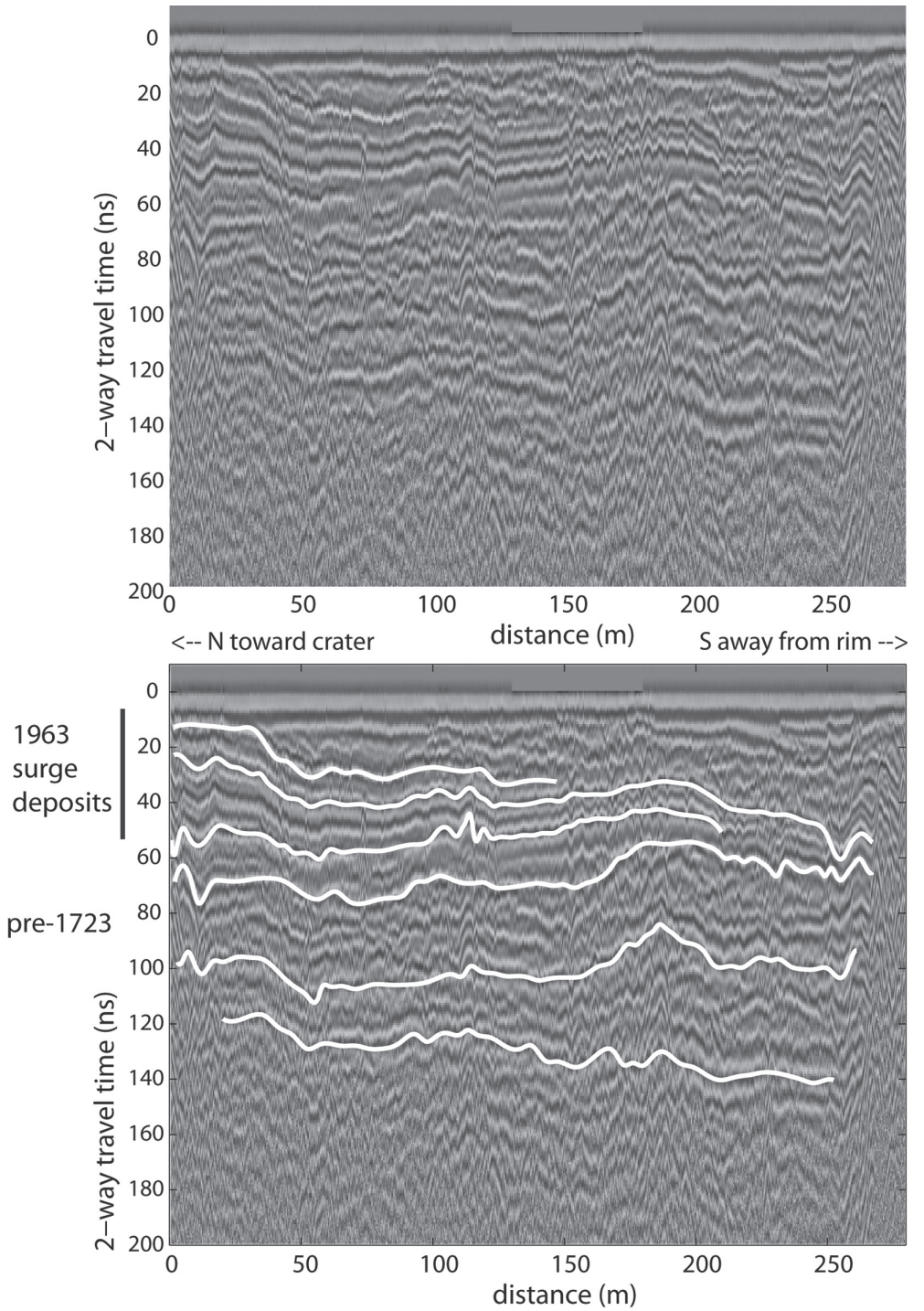

Fig. 9: GPR Profile C on Irazú "Rim Deposits". Location shown on Figure 4. Top: uninterpreted GPR profile: left end is on crater rim, right end is to the south near the caldera rim. Bottom: Selected radar horizons were picked for analysis. Stratigraphic interpretation is based on field observations and correlations with rim deposits described in Alvarado (1993).

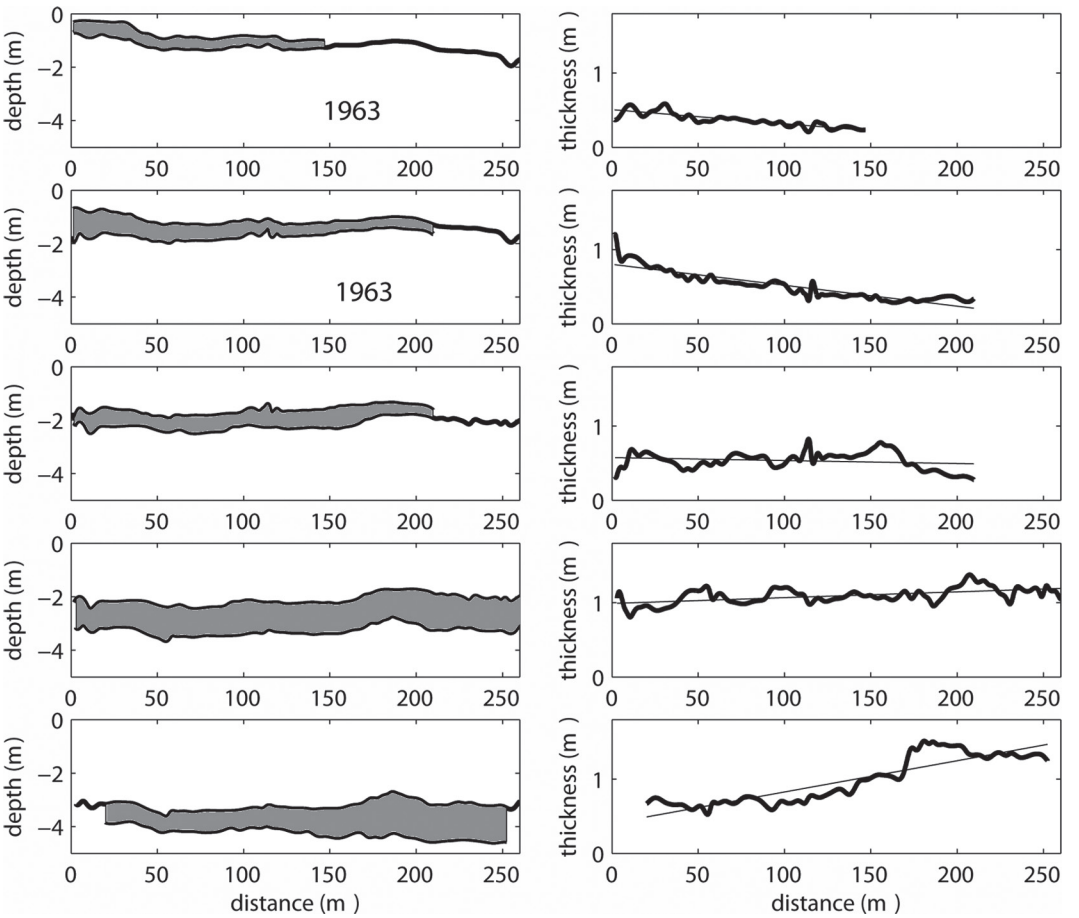

Fig. 10: Thicknesses of Irazú rim deposit packages between the 6 radar horizons identified in Figure 9. The 1963 surge deposits thin consistently with distance from the crater rim (to the right, or south). Older packages (1723 and older) show uniform thicknesses or increasing thickness with distance from crater rim, suggesting reworking or reverse flow of surges returning from the caldera wall.

Of the 5 packages between the 6 selected contacts, the uppermost two consist of surge deposits associated with 1963 eruptions. Both thin consistently with distance from the crater rim (right column, Figure 10) by about at rates of about 1-2 mm per meter of radial distance. The radar records also indicate that these surge deposits general follow pre-existing topography rather than infilling topographic lows. In contrast, the surficial units overlying the shallowest identified package thicken irregularly with distance from crater rim. These deposits are presumed to be erosional products. There are clear indications in the form of shallow surficial channels that erosion has modified 1963-65 playa deposits. Transport is toward a topographic depression marked by a small ephemeral lagoon in the central part of the Playa Hermosa (Figure 4).

In contrast to the 1963 surge units, older packages are relatively uniform in thickness or increase slightly in thickness away from the crater rim (Figure 10). Alvarado (1993) noted such relationships in stream cuts at the western edge of Playa Hermosa, and suggested these thickness relationships may represent reworking of rim deposits as well as reverse flow of some surges back from the caldera rim.

The GPR data also shed light on the mechanics of deposition of blocks and bombs. For example, Figure 11 shows that a large block can be identified at 3.5 m depth (100 ns two-way travel

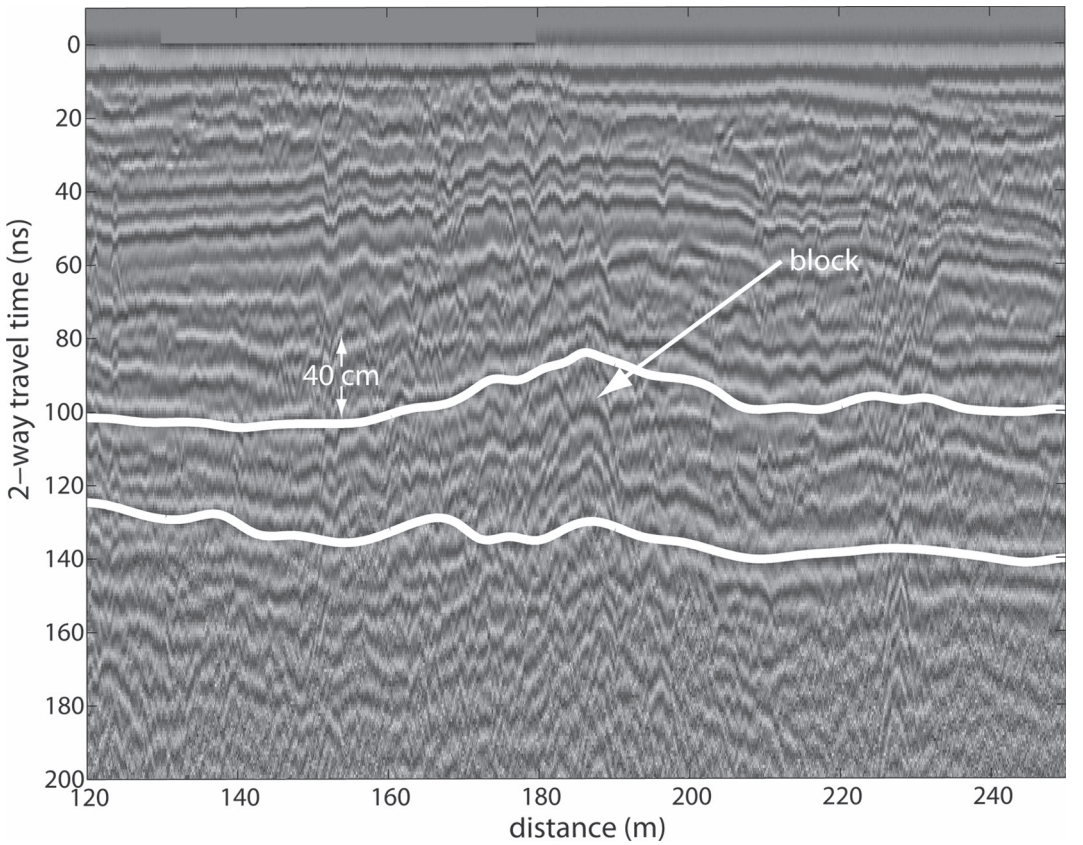

Fig. 11: Example of draping of deposits over a block with dimension approximately 40 cm on Irazu's Playa Hermosa. From Profile C (location in Figure 4). The block itself appears as a diffraction hyperbola; younger deposits clearly drape this feature.

time) at a distance of ~180 m from the crater rim. The block itself appears clearly in the radar record as a diffraction pattern. Overlying units are clearly draped over this block, which locally thickens the package by 40 cm (Figure 11). In this example it is not clear whether underlying strata sag under the block. However, it is clear that for blocks in the 1963 surge deposits, the blocks induce a sag in the underlying layer, as the peak of the diffraction appears lower in the record than adjacent reflecting boundaries (examples in Figure 12).

DISCUSSION AND CONCLUSIONS

On Poás and Irazú volcanoes, GPR was demonstrated to be a useful tool for mapping stratigraphic packages between exposures in stream cuts, trenches, and outcrops. The antenna frequencies used in the test profiles presented here (100 MHz and 200 MHz) typically cannot resolve individual ash or surge deposits, but yield useful images of the attitude and structure of beds. On both volcanoes, GPR successfully images clasts, blocks and bombs with dimensions on the order of 5 cm or more in the uppermost few meters, but resolution of these features decreases with depth (and with lower antenna and signal frequency).

GPR was particularly successful on both Poás and Irazú on near-vent deposits within 100s of m of the active crater. On the near-vent deposits GPR spatial resolution was >~ 10 cm, with depth of penetration ~6-20 m. The profile with the least stratigraphic information came from the most distal site on Poás, where deposits lacked the clear

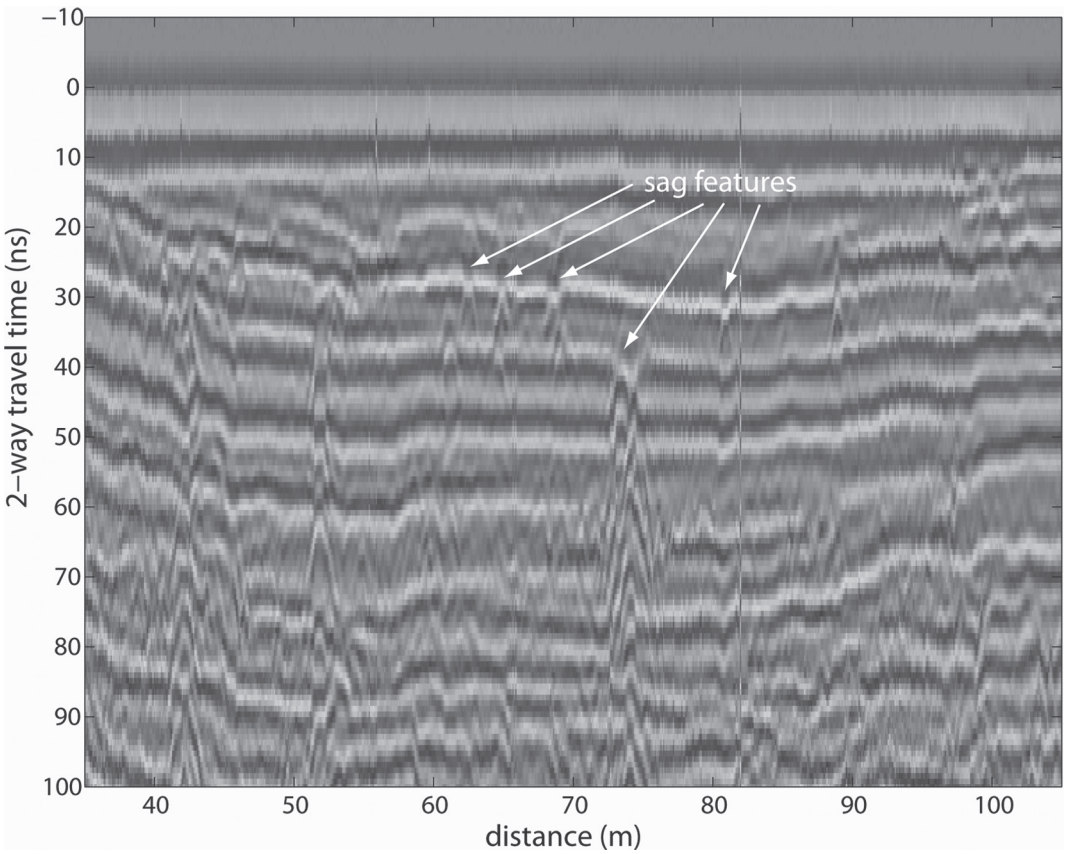

Fig. 12: Within the 1963 surge deposits on Irazu's Playa Hermosa are numerous diffractions with peaks just below the level of nearby reflecting horizons. These results show that the blocks causing the radar diffractions produced sags in the horizons onto which they were deposited. From Profile C (location in Figure 4).

stratification in porosity observed at the near-vent sites. Spatial resolution was enhanced on wet days when the velocity was lower, and radar wavelength shorter.

We note that considerably more geologic information could be extracted from the Irazú profiles because they are longer and because the there were more nearby outcrops available and studied. Irazú also offers much more accessible terrain than Poás, as vegetative regrowth over deposits from the 1963-1965 Irazú eruption sequence is still limited. On Irazú, a strong radar return correlates well with the base of the 1963 deposits. Profiles also show internal structure within the intracrater explosive units (ICEUs) of the 1963-1965 eruptive sequence mapped by Alvarado (1993). Changes in layer thickness with distance from the crater rim (over many tens of meters) were interpreted to correspond to surge deposits, including both forward and reverse flow events. Volcanic blocks and sag features are clearly identified, as well as post-eruptive mobilization of surficial deposits.

On Poás volcano GPR profiles show distinctive returns, including a horizon that may represent an unconformity between better consolidated and less consolidated tephra deposits. However little is known about the pre-1910 deposits that represent the bulk of the radar images at the Poás trench site, and further profiling with 200 MHz antennas was thus deemed of little utility. Clearly higher frequency antennas with better spatial resolution (500 MHz – 1 GHz) could be useful for tracking the 1910 and subsequent ash deposits,

particularly because outcrops on Poás flanks are scarce and historical deposits are thin (<~2 m).

ACKNOWLEDGEMENTS

S. Kruse thanks the Escuela Centroamericana de Geología of the Universidad de Costa Rica for logistical support for this project. We are grateful to Maritta Alvarado, Helen Aguilar, and Thomas Juster for help in the field. Mitchell Craig provided a very constructive review of the manuscript.

REFERENCES

ALVARADO INDUNI, G.E., 1993: Volcanology and Petrology of Irazú Volcano, Costa Rica.- 261 págs. Christian-Albrechts-Universität, Kiel [Tesis Ph.D.].

ALVARADO, G.E., CARR, M.J., TURRIN, B.D., SWISHER, C.C., SCHMINCKE, H.-U. & HUDNUT, K.W., 2006: Recent volcanic history of Irazú volcano, Costal Rica: Alternation and mixing of two magma batches, and pervasive mixing.- In: ROSE, W.I., BLUTH, G.J.S., CARR, M.J., EWERT, J., PATINO, L.C., & VALLANCE, J. (eds): Volcanic hazards in Central America.- Geol. Soc. of America Spec. Paper, 412: 259–276. DOI: 10.1130/2006.2412(14).

CAGNOLI, B. & RUSSELL, J.K., 2000: Imaging the subsurface stratigraphy in the Ubahebe hydrovolcanic field (Death Valley, California) using ground penetrating radar.- J. Volcanol. and Geother. Res. 96: 45-56.

CAGNOLI, B. & ULRYCH, T.J., 2001a: Downflow amplitude decrease of ground penetrating radar reflections in base surge deposits.- J. Volcanol. and Geother. Res. 105: 25-34.

CAGNOLI, B. & ULRYCH, T.J., 2001b: Ground penetrating radar images of unexposed climbing dune-forms in the Ubahebe hydrovolcanic field (Death Valley, California).- J. Volcanol. and Geother. Res. 109: 279-298.

CHOW, J.J., CHANG, S.-K. & YU, H.-S., 2006: GPR reflection characteristics and depositional models of mud volcanic sediments—Wushanting mud volcano field, southwestern Taiwan.- J. Applied Geophys. 60: 179-200.

GÓMEZ-ORTIZ, D., MARTÍN-VELÁZQUEZ, S. , MARTÍN-CRESPO, T., MÁRQUEZ, A., LILLO, J., LÓPEZ, I. & CARREÑO, F., 2006: Characterization of volcanic materials using ground penetrating radar: A case study at Teide volcano (Canary Islands, Spain).- J. Applied Geophys. 59: 63-78.

GRIMM, R. E., HEGGY, E., CLIFFORD, S., DINWIDDIE, C., MCGINNIS, R., & FARRELL, D., 2006: Absorption and scattering in ground-penetrating radar: Analysis of the Bishop Tuff.- J. Geophys. Res. 111, E06S02. DOI:10.1029/2005JE002619.

GUHA, S., KRUSE, S.E., WRIGHT, E.E. & U.E. KRUSE, 2005: Spectral analysis of ground penetrating radar response to thin sedimentary layers.- Geophys. Res. Lett. 32: L23304. DOI: 10.1029/2005GL023933.

HEGGY, E., CLIFFORD, S.M., GRIMM, R.E., DINWIDDIE, C.L., WYRICK, D.Y. & HILL, B.E., 2006: Ground-penetrating radar sounding in mafic lava flows: Assessing attenuation and scattering losses in Mars-analog volcanic terrains.- J. of Geophys. Res. 111, E06S04. DOI: 10.1029/2005JE002589.

IRVING, J.D. & KNIGHT, R.J., 2003: Removal of wavelet dispersion from ground-penetrating radar data.- Geophysics, 63(3): 960-970.

MIYAMOTO, H., HARUYAMA, J., KOBAYASHI, T., SUZUKI, K., OKADA, T., NISHIBORI, T., SHOWMAN, A.P., LORENZ, R., MOGI, K., CROWN, D.A., RODRIGUEZ, J.A.P., ROKUGAWA, S., TOKUNAGA, T. & MASUMOTO, K., 2005: Mapping the structure and depth of lava tubes using ground penetrating radar.- Geophys. Res. Lett. 32, L21316. DOI:10.1029/2005GL024159.

MORA-AMADOR, R., 2010: Peligrosidad volcánica del Poás (Costa Rica), basado en las principales erupciones históricas de 1834, 1910 y 1953-1955.- 111 págs. Univ. Costa Rica San José, [Tesis M.Sc.].

RUDÍN, J., ALFARO, A., MICHAUD G., RUDÍN, A., 1910: Gran erupción de cenizas del volcán Poás. In VARGAS, C.A., 1979: Antología Volcán Poás.- 162 págs. EUNED, San José.

MONESTEL, Y., 2004. Notas sobre la erupción de mayo de 1953 en el volcán Poás. [Inédito].

RUSSELL, J.K. & STASIUK, M.V., 1997: Characterization of volcanic deposits with ground-penetrating radar.- Bull. Volcanol. 58: 515-527.

RUST, A.C. & RUSSELL, J.K., 2000: Detection of welding in pyroclastic flows with ground penetrating radar: insights from field and forward modeling data.- J. Volcanol. and Geother. Res. 95: 23-34.

RUST, A.C. & RUSSELL, J.K., 2001: Mapping porosity variation in a welded pyroclastic deposit with signal and velocity patterns from ground-penetrating radar surveys.- Bull. Volcanol. 62: 457-463.

STOCKWELL, R.G., MANSINHA, L. & LOWE, R.P., 1996: Localization of the Complex Spectrum: The S Transform.- IEEE Trans. on Signal Processing, 44(4): 998-1001.